Water Research 159 (2019) 102–110

Contents lists available at ScienceDirect

Water Research

journal homepage: www.elsevier.com/locate/watres

The individual and Co-exposure degradation of benzophenone derivatives by UV/H_2O_2 and UV/PDS in different water matrices

Jinming Luo [a], Tongcai Liu [b, c], Danyu Zhang [c], Kai Yin [b, c, *], Dong Wang [a], Weiqiu Zhang [a], Chengbin Liu [c], Chunping Yang [b], Yuanfeng Wei [c], Longlu Wang [b, c], Shenglian Luo [c], John C. Crittenden [a]

[a] Brook Byers Institute for Sustainable Systems and School of Civil and Environmental Engineering, Georgia Institute of Technology, 828 West Peachtree Street, Atlanta, GA 30332, United States
[b] College of Environmental Science and Engineering, Hunan University, Changsha, 410082, PR China
[c] State Key Laboratory of Chemo/Biosensing and Chemometrics, Hunan University, Changsha, 410082, PR China

ARTICLE INFO

Article history:
Received 30 January 2019
Received in revised form
11 April 2019
Accepted 5 May 2019
Available online 6 May 2019

Keywords:
UV filters
Advanced oxidation processes
Reactive nitrogen/halogen species
Feeding pattern

ABSTRACT

Benzophenone derivatives, including benzophenone-1 ($C_{13}H_{10}O_3$, BP1), benzophenone-3 ($C_{14}H_{12}O_3$, BP3) and benzophenone-8 ($C_{14}H_{12}O_4$, BP8), that used as UV filters are currently viewed as emerging contaminants. Degradation behaviors on co-exposure benzophenone derivatives using UV-driven advanced oxidation processes under different aqueous environments are still unknown. In this study, the degradation behavior of mixed benzophenone derivatives via UV/H_2O_2 and UV/peroxydisulfate (PDS), in different water matrices (surface water, hydrolyzed urine and seawater) were systematically examined. In surface water, the attack of BP3 by hydroxyl radicals (HO•) or carbonate radicals ($CO_3^{\bullet-}$) in UV/H_2O_2 can generate BP8, which was responsible for the relatively high degradation rate of BP3. Intermediates from BP3 and BP8 in UV/PDS were susceptible to $CO_3^{\bullet-}$, bringing inhibition of BP1 degradation. In hydrolyzed urine, Cl^- was shown the negligible effect for benzophenone derivatives degradation due to low concentration of reactive chlorine species (RCS). Meanwhile, BP3 abatement was excessively inhibited during co-exposure pattern. In seawater, non-first-order kinetic behavior for BP3 and BP8 was found during UV/PDS treatment. Based on modeling, Br^- was the sink for HO•, and the co-existence of Br^- and Cl^- was the sink for $SO_4^{\bullet-}$. The cost-effective treatment toward target compounds removal in different water matrices was further evaluated using EE/O. In most cases, UV/H_2O_2 process is more economically competitive than UV/PDS process.

1. Introduction

To protect humans from the harmful effects of ultraviolet radiation, UV filters are used in a diverse range of personal care products (PCPs), including sunscreens, cosmetics and shampoo (Fent et al., 2010; Jansen et al., 2013). UV filters are used in combinations and can exceed 10% of the product's mass (Brausch and Rand, 2011; Schreurs et al., 2002). Among UV filters, benzophenone derivatives are commonly used due to their high photo/biostability, resulting in their general occurrence in environment media, especially aqueous environments (Brausch and Rand, 2011; Kasprzyk-Hordern et al., 2008; Poiger et al., 2004; Tsui et al., 2017). Due to their endocrine disrupting potential and carcinogenic effects, benzophenone derivatives are considered to the emerging contaminants in recent decades (Schlumpf et al., 2001; Schreurs et al., 2005; Suzuki et al., 2005; Tang et al., 2013). The most detected UV filters families in surface water were benzophenone derivatives with concentrations up to 0.4 mg/L (Kasprzyk-Hordern et al., 2009). Meanwhile, benzophenone-1 ($C_{13}H_{10}O_3$, BP1) and benzophenone-8 ($C_{14}H_{12}O_4$, BP8) in the influent of urban sewage treatment plants have reached maximum concentrations of 245 and 10 ng/L, respectively (Negreira et al., 2009; Wu et al., 2013). Benzophenone-3 ($C_{14}H_{12}O_3$, BP3) has been reported to occur in surface waters in Switzerland, at a concentration range of <2–35 ng/L (Balmer et al., 2005), and in wastewater from China, at concentration ranging from 68 to 722 ng/L (Li et al., 2007). Besides, UV filters were also

* Corresponding author. College of Environmental Science and Engineering, Hunan University, Changsha, 410082, PR China.
E-mail address: yinkai@hnu.edu.cn (K. Yin).

https://doi.org/10.1016/j.watres.2019.05.019
0043-1354/

detected in seawater (Tsui et al., 2017; Manasfi et al., 2017), even in human urine because of dermal exposure (Kunisue et al., 2012; Wang et al., 2013). Hence, an efficient and economical approach to removing these pollutants from aquatic environments is highly needed.

Advanced oxidation processes (AOPs), which can generate reactive species, are becoming increasingly popular technologies for contaminants degradation in water (Oller et al., 2011; Oturan and Aaron, 2014). Radical-based AOPs, in particular those with hydroxyl radical (HO•) or sulfate radical ($SO_4^{\bullet-}$), have been successfully applied to decompose micropollutants (Keen and Linden, 2013; Luo et al., 2015, 2017; Nfodzo and Choi, 2011; Yang et al., 2019; Liu et al., 2018). Meanwhile, AOPs were also used in human urine and seawater to obtain the pharmaceuticals removal, toxicity elimination and disinfection (Zhang et al., 2015, 2016b; Rubio et al., 2013). Reports have shown that many micropollutants can react rapidly with HO• ($10^8 \leq k \leq 10^{10}\ M^{-1}\ s^{-1}$) (Wols and Hofman-Caris, 2012), whereas the reaction rates of PCPs with HO• and $SO_4^{\bullet-}$ have not been extensively studied, especially for secondary reactive species (i.e., carbonate radical-$CO_3^{\bullet-}$). Additionally, one critical issue is that micropollutants, such as PCPs, normally occur in a co-exposure pattern rather than individual existence in aqueous environments. The degradation behaviors of PCPs in co-exposure pattern are likely different from individual pattern using AOPs. However, the specific difference of degradation behaviors and its related factors for triggering are still unknown. Furthermore, constituents in various water matrices make micropollutants degradation even more complex because of conversions of reactive species (Yang et al., 2014; Zhang et al., 2015). To the best of our knowledge, degradation behaviors of multiple PCPs (i.e., UV filters) by AOPs in various aqueous environments have not been investigated.

In this study, the degradation of benzophenone derivatives in both individual and co-exposure patterns by UV/H_2O_2 and UV/PDS in the presence of different water matrices (surface water, hydrolyzed urine and seawater) was comprehensively investigated. The degradation kinetics were also experimentally and mathematically determined. For the first time, the reaction rate constants of benzophenone derivatives toward HO•, $SO_4^{\bullet-}$ and $CO_3^{\bullet-}$ were determined, which can largely benefit the future work regarding on the kinetic simulation of radical-based degradation in other water matrices. An energy-cost evaluation (i.e., electrical efficiency per log order (EE/O)) was also conducted to compare the energy cost of UV-based AOPs in different water matrices.

2. Materials and methods

2.1. Chemicals and reagents

Sources of chemicals, reagents and synthetic matrices were provided in the Supporting Information Text S1 and Tables S1-S2.

2.2. Kinetics of UV filter oxidation by UV/H_2O_2 and UV/PDS in different water matrices

A semi-collimated beam apparatus (Figure S1) consisting of one 15-W low-pressure mercury lamp above a quartz reactor (6 cm diameter × 5 cm height) was employed for batch studies. Kinetics experiments were conducted at room temperature (25 ± 1 °C) in aqueous solutions, including ultrapure water with phosphate buffer solution (PBS), surface water, hydrolyzed urine and seawater (Tables S2). The volumetric light irradiance (I, $1.99 \times 10^{-6}\ E\ L^{-1}\ s^{-1}$) was determined by H_2O_2 chemical actinometry (Beltrán et al., 1995; Yin et al., 2018). All kinetics experiments were performed twice at least.

2.3. Determination of second-order rate constants of UV filters with HO•, $SO_4^{\bullet-}$ and $CO_3^{\bullet-}$

Competition kinetic approaches were used to determine the second-order rate constants of UV filters with HO•, $SO_4^{\bullet-}$ and $CO_3^{\bullet-}$, using nitrobenzene (NB), anisole (AS) and *para*-nitroaniline (PNA) as reference compounds, respectively. $CO_3^{\bullet-}$ was generated by adding excess sodium bicarbonate (0.5 M) during UV/H_2O_2 process. The experiments were conducted in PBS at pH 7 (for HO• and $SO_4^{\bullet-}$) and pH 9 (for $CO_3^{\bullet-}$). The initial concentrations of UV filters and oxidants were 5 μM and 500 μM, respectively. In addition, the concentrations of NB, AS and PNA were 5 μM, 50 μM and 5 μM, respectively.

2.4. Chemical analysis

A HITACHI L-2130 HPLC equipped with an Inert Sustain C18 column (4.6 mm × 250 mm, 5 μm particle size) and L-2420 UV–Vis detector was used to quantify UV filters. The column temperature was set at 35 °C. The eluent was methanol (0.1% acetic acid)/purified water (v/v, 80/20); flow rate was 1 mL/min. The injection volume was 10 μL for each sample, and UV detection was set at 290 nm. Detection wavelengths for NB, AS and PNA were set at 275, 270 and 220 nm, respectively.

The transformation products of UV filters were identified by HPLC coupled triple quadrupole MS (tqMS) (Agilent Technology 1290/6460 Triple Quad LC/MS) with electro spray ionization (ESI) operating in positive mode. Solid phase extraction (SPE) for samples pretreatment (Text S1) were performed to avoid the possible contamination of mass spectrometer by inorganic ions. A ZORBAX Eclipse Plus C18 (2.1 × 50 mm, 1.8 μm and 600 Bar) was used for separation with a mobile phase composed of methanol and water (65:35, v/v) with flow rate of 0.2 mL/min. The mass spectrometer was operated at fragmentation voltage 135 V, capillary voltage 140 V, gas temperature 350 °C and nebulizer pressure 35 psi. The exact mass information of transformation products were illustrated by using LTQ-Orbtirap Velos Pro. The sheath gas flow rate was 8 arb, spay voltage 4.5 kV, and capillary temperature 275 °C. The analyzer, mass range and resolution of scan description was FTMS, *m/z* 100–500 and 60000, respectively.

2.5. Kinetic modeling

Radical concentrations in UV/H_2O_2 and UV/PDS systems were simulated using Kintecus 4.55 to evaluate the reactive species (Ianni, 2012). The virtues of Kintecus runs incredibly fast on personal computer and is basically unrestricted in terms of the number of reactions and species. Further, the program automatically checks for correct mass and charge balance and also offers the opportunity to modify the concentrations of selected compounds at any point during time scale. This feature easily allows modeling the actual conditions of experiments. More than two hundred elementary reactions (Tables S3) were involved. This model accounts for the effects of most inorganic ions, including chloride, sulfate, carbonate species and bromide on UV/H_2O_2 and UV/PDS, and it has been successfully employed in several studies with proven reliability for simulations (Sun et al., 2016; Yang et al., 2014; Zhang et al., 2015, 2016a).

3. Results and discussion

3.1. Direct photolysis

Direct photolysis (UV alone) of individual (BP1, BP3 and BP8 for individual substance, hereafter referred to as BP) and co-exposure

(referred to BPs) benzophenone derivatives were studied in ultrapure water with PBS. After 60 min irradiation, the degradation of BP and BPs were not evidently observed (Figure S2), confirms their photo-stability. These results were consistent with previous study, which also did not observe BP3 photo-degradation under UV irradiation (Liu et al., 2011). Meanwhile, no degradation of BP was observed after 60 min with either H_2O_2 or PDS in the absence of light (Figure S2), indicating that the degradation role of oxidants can be neglected. Therefore, in this study, this discussion focuses on photolysis via photo-generated reactive species in different matrices.

3.2. UV/H_2O_2 and UV/PDS AOPs in ultrapure water

Kinetic modeling was combined with experiments to comprehensively illustrate how the target compounds degradation was driven by different radicals, rather than to draw a definitive conclusion on the concentration of radical. In UV/H_2O_2 and UV/PDS, the overall degradation is owing to both direct and indirect photolysis (Eq. (1)):

$$-\frac{d[BP]}{dt} = k_{obs}[BP] = (k_d + k_i)[BP] \approx k_i[BP] \quad (1)$$

where k_{obs} is the observed pseudo-first-order degradation rate constant (min^{-1}); k_d is the measured pseudo-first-order direct photolysis rate constant (min^{-1}); and k_i is the indirect photolysis rate constant (min^{-1}) and is primarily related to reactive species. Due to negligible direct photolysis (Figure S2), the k_{obs} equals to the indirect photolysis rate k_i in UV/H_2O_2 or UV/PDS.

BP was treated by UV with either 500 μM of H_2O_2 or PDS at pH 7.2. The photolysis rate of BP followed pseudo-first-order kinetics (Figure S3). In ultrapure water, k_{obs} of BP1, BP3 and BP8 were increased from 0 to 0.214, 0.278 and 0.348 min^{-1}, respectively, by UV/H_2O_2. The increase of k_{obs} was primarily due to the contribution of HO·. A competition kinetic method (Text S2) was used to determine the second-order rate constants of BP with HO· ($k_{HO\cdot}$, Table 2), which were in a narrow range (6.25×10^9 to 7.05×10^9 M^{-1} s^{-1}) due to low selectivity of HO·. A higher $k_{HO\cdot}$ led to a higher degradation rate of BP (Fig. 1A). Furthermore, degradation results from BPs treatment by UV/H_2O_2 showed that each contaminant followed pseudo-first-order kinetics (Figure S3D). To be noted, the degradation rate in co-exposure pattern followed the order BP3 < BP8 < BP1, which differs from individual pattern (BP1 < BP3 < BP8). This result indicates that some interference may occurred during co-exposure. The different degradation orders of individual and co-exposure patterns may relate to molecular structure, byproducts generated and treatment technique, indicating that further study was needed.

Table 2
Second-order rate constants[a] of the compounds with hydroxyl, sulfate and carbonate radicals determined in pH 7 and 9 PBS.

	pH 7		pH 9		
	$k_{HO\cdot}$ ($\times 10^9$)	$k_{SO4\cdot-}$ ($\times 10^{10}$)	$k_{HO\cdot}$ ($\times 10^9$)	$k_{SO4\cdot-}$ ($\times 10^{10}$)	$k_{CO3\cdot-}$ ($\times 10^7$)
BP1	6.25 (±0.25)	1.68 (±0.34)	6.75 (±0.31)	1.13 (±0.40)	3.28 (±0.51)
BP3	6.94 (±0.20)	2.60 (±0.25)	7.38 (±0.35)	1.56 (±0.49)	1.25 (±0.23)
BP8	7.05 (±0.17)	2.77 (±0.29)	7.46 (±0.23)	1.23 (±0.33)	2.79 (±0.45)

[a] All the rate constants unit = M^{-1} s^{-1}, errors represent standard deviation (n ≥ 2).

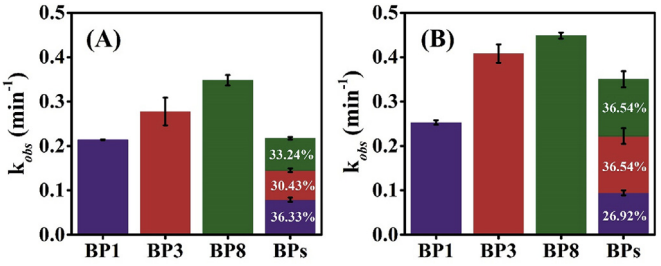

Fig. 1. Measured the degradation rate constants (k_{obs}) of BP1, BP3, BP8 and BPs in PBS (10 mM) at pH 7.2 by UV/H_2O_2 (A) and UV/PDS (B). Reaction condition: [BP1] = [BP3] = [BP8] = 5 μM, [H_2O_2] = [PDS] = 500 μM, I = 1.99×10^{-6} E L^{-1} s^{-1} and temperature at 25 ± 1 °C. Errors represent the standard deviation (n ≥ 2).

Compared with UV/H_2O_2, UV/PDS in ultrapure water led to faster BP degradation, but to different extents (Fig. 1B). The second-order rate constants of BP with $SO_4^{\cdot-}$ ($k_{SO4\cdot-}$) were determined using competition kinetic (Text S2), which were 1.68, 2.60 and 2.77×10^{10} M^{-1} s^{-1} for BP1, BP3 and BP8, respectively (Table 2). k_{obs} of BP1, BP3 and BP8 in UV/PDS were 0.253, 0.408 and 0.448 min^{-1}, respectively. All these values were higher than those observed when using UV/H_2O_2. The enhanced degradation of BP in UV/PDS was mainly attributed to the formation rate of $SO_4^{\cdot-}$ from PDS ($\Phi_{PDS} = 0.7$) was higher than that of HO· from H_2O_2 ($\Phi_{H2O2} = 0.5$) (Baxendale and Wilson, 1957; Mark et al., 1990). The degradation rates in co-exposure pattern using UV/PDS followed the order BP1 < BP3 = BP8, which also differs from individual system (BP1 < BP3 < BP8). In co-exposure pattern, k_{obs} for BP1, BP3 and BP8 in UV/PDS were 0.094, 0.128 and 0.128 min^{-1}, respectively, higher

Table 1
Simulated molar concentration (in M) of inorganic radicals for various model water matrices.[a].

Reactive species	UV/H_2O_2				UV/PDS			
	Ultrapure water	Surface water	Hydrolyzed urine	Seawater	Ultrapure water	Surface water	Hydrolyzed urine	Seawater
[$SO_4^{\cdot-}$]					2.54×10^{-12}	1.87×10^{-13}	2.94×10^{-15}	6.22×10^{-16}
[HO·]	5.00×10^{-12}	5.05×10^{-13}	1.62×10^{-15}	1.04×10^{-14}	1.33×10^{-11}	1.46×10^{-13}	3.96×10^{-18}	1.10×10^{-15}
[Cl·]			5.96×10^{-23}	2.81×10^{-18}			9.77×10^{-17}	2.78×10^{-17}
[ClO·]			4.03×10^{-36}	4.44×10^{-21}			1.39×10^{-21}	1.68×10^{-12}
[Br·]				1.10×10^{-14}				2.24×10^{-14}
[$Cl_2^{\cdot-}$]			8.56×10^{-21}	3.66×10^{-15}			4.31×10^{-15}	3.62×10^{-14}
[$ClBr^{\cdot-}$]				6.59×10^{-12}				1.31×10^{-11}
[$Br_2^{\cdot-}$]				1.85×10^{-11}				3.67×10^{-11}
[$CO_3^{\cdot-}$]		1.44×10^{-11}	2.41×10^{-13}	1.22×10^{-10}		5.83×10^{-12}	3.09×10^{-12}	7.87×10^{-12}
[$\cdot NH_2$]			3.37×10^{-13}				2.93×10^{-13}	
[$\cdot NO_2$]			1.49×10^{-16}				1.18×10^{-30}	
[·NO]			2.32×10^{-5}				2.06×10^{-5}	
[ONOOH]			1.09×10^{-11}				7.65×10^{-26}	
[$ONOO^-$]			1.22×10^{-10}				8.57×10^{-25}	

[a] Oxidant concentration was 500 μM; the contaminants were not included in the system when performing the calculation; total simulation time was 3 min.

than those obtained in UV/H_2O_2. Meanwhile, the overall k_{obs} of BPs for UV/PDS was 1.61 times higher than that for UV/H_2O_2. Therefore, UV/PDS treatment demonstrated higher degradation efficiency for the abatement of target compounds.

Overall, results show that UV/PDS in ultrapure water was more efficient than UV/H_2O_2 for both individual and co-exposure patterns. However, whether this conclusion can be applied in real matrices need further investigation. The presence of diverse constituents in actual environments and conversion of reactive species can further complicate these contaminants elimination. Additionally, degradation behavior of target contaminants could be distinct for different feeding patterns, representing a topic that has not been previously examined in a systematic manner. This research is significant demanded because of the coexistence of constituents and multiple benzophenone derivatives in aquatic environments. Therefore, three typical water matrices, including surface water, hydrolyzed urine and seawater, were selected for further studies owing to UV filters occurrence (Asimakopoulos et al., 2014; Cuderman and Heath, 2007; Kim and Choi, 2014; Magi et al., 2013; Manasfi et al., 2015; Meeker et al., 2013; Philippat et al., 2012; Tsui et al., 2014).

3.3. UV/H_2O_2 and UV/PDS AOPs in surface water

Compared to ultrapure water, k_{obs} for BP1, BP3 and BP8 using UV/H_2O_2 decreased by 46.24, 51.50 and 58.37%, respectively, in surface water (Fig. 2A). Kinetic modeling indicated that HO· concentration decreased to 5.05×10^{-13} M in surface water compared to that in ultrapure water (5.00×10^{-12} M, Table 1). The decrease in HO· concentration was primarily due to competing reactions with natural organic matter (NOM) and bicarbonate (HCO_3^-). The second-order rate constants of NOM with HO· and $CO_3^{\cdot-}$ have been reported as 3.9×10^8 $M_c^{-1} \cdot s^{-1}$ and 2.3×10^4 $M_c^{-1} \cdot s^{-1}$, respectively (Brezonik and Fulkerson-Brekken, 1998; Canonica et al., 2005). High concentration and reactivity toward radicals made NOM become the major scavenger in surface water.

The k_{obs} for BP was inhibited by less than 60%, which indicated that BP degradation was not only governed by HO·. The k_{obs} in surface water should have been approximately 10% of that in ultrapure water if only HO· oxidation was considered (Table 1). This discrepancy suggests that $CO_3^{\cdot-}$ was also responsible for BP degradation. The second-order rate constants of BP with $CO_3^{\cdot-}$ ($k_{CO_3^{\cdot-}}$) were also determined (Text S2), and it revealed that $CO_3^{\cdot-}$ exhibited lower reactivity than HO· (Table 2). Compared with other contaminants, whose second-order rate constants with $CO_3^{\cdot-}$ were approximately 10^6-10^7 M^{-1} s^{-1} (Wols et al., 2015), BP was highly reactive toward $CO_3^{\cdot-}$ (1.25×10^7 to 3.28×10^7 M^{-1} s^{-1}) because of its electron-rich moieties. Although $k_{CO_3^{\cdot-}}$ was at least two orders of magnitude lower than that of $k_{HO\cdot}$, the higher selectivity of $CO_3^{\cdot-}$ also rendered it less susceptible to be scavenged by constituents (Zhang et al., 2016a). This lower susceptibility was evident from modeling, which showed that the concentration of $CO_3^{\cdot-}$ was almost 30 times higher than that of HO· in surface water (Table 1 and S5).

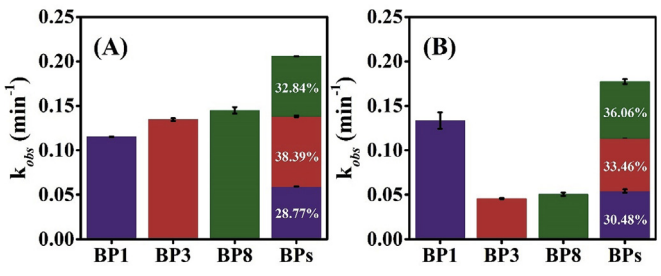

Fig. 2. Measured the degradation rate constants (k_{obs}) of BP1, BP3, BP8 and BPs in surface water at pH 7.2 by UV/H_2O_2 (A) and UV/PDS (B). Reaction condition: [BP1] = [BP3] = [BP8] = 5 μM, [H_2O_2] = [PDS] = 500 μM, $I = 1.99 \times 10^{-6}$ E L^{-1} s^{-1} and temperature at 25 ± 1 °C. Errors represent the standard deviation (n ≥ 2).

In UV/PDS-treated surface water, k_{obs} of BP also experienced a strong suppression, especially for BP3 and BP8 (Fig. 2B). Given electrophilic nature of $CO_3^{\cdot-}$ (Liu et al., 2015), aromatic contaminants with electron-donating substituents are also reactive toward $CO_3^{\cdot-}$, similar to HO· and $SO_4^{\cdot-}$. Two hydroxyl groups (-OH) on BP1 can activate benzene ring, which explains why BP1 demonstrates higher reactivity than BP3 and BP8. Likewise, k_{obs} should approach zero if degradation was only governed by $SO_4^{\cdot-}$ and HO·, further confirming the participation of $CO_3^{\cdot-}$ in BP degradation. When surface water was treated by UV/PDS, a higher degradation rate for BP1 and lower degradation rates for BP3 and BP8 can be observed compare to UV/H_2O_2. Based on the simulated $SO_4^{\cdot-}$ and HO· concentrations (Table 1) and measured rate constants (Table 2), UV/PDS was expected to have better performance on BP degradation than UV/H_2O_2. However, this hypothesis was only true for BP1 (Fig. 2). A lower concentration of $CO_3^{\cdot-}$ (Table 1) and $k_{CO_3^{\cdot-}}$ played a critical role in the degradation of BP3 and BP8. Further study is necessary to determine whether any underestimated rate constant for the reaction with (or unknown scavenger of) $SO_4^{\cdot-}$, which can resulted in a lower concentration than predicted result.

When BPs were added to surface water and treated using UV/H_2O_2 and UV/PDS, degradation followed pseudo-first-order kinetics (Figure S5D and S6D). Interestingly, the overall k_{obs} for BPs treated with UV/H_2O_2 (0.206 min^{-1}) exceeded that of UV/PDS (0.178 min^{-1}) (Fig. 2). The order of degradation for BPs via UV/H_2O_2 was BP1 < BP8 < BP3, which was different from that in individual system (BP1 < BP3 < BP8). One possible explanation for this difference was that BP3 may transform into BP8 via (i) hydrogen abstraction by HO· or (ii) electron transfer from HO· and $CO_3^{\cdot-}$ (Scheme 1). This hypothesis was verified by BP8 appearance when BP3 was treated using UV/H_2O_2 (Figure S7). The HO-byproducts generated could be detected as well for different model compounds using UV/H_2O_2 (Yao et al., 2013; Feng et al., 2015; Castro et al., 2016; Zhang et al., 2016b; Yin et al., 2018). A suppression of BP1 by UV/PDS in co-exposure pattern might suggest the conversion of BP3 to BP1, similarly via cytochrome P450 enzymes (Nakagawa and Suzuki, 2002). However, it was disregarded because of the absence of BP1 when BP3 was treated using UV/PDS. A possibility existed that intermediates from BP3 or/and BP8 were susceptible to $CO_3^{\cdot-}$ attack, which leading to the suppression of BP1.

3.4. UV/H_2O_2 and UV/PDS AOPs in hydrolyzed urine

Recovering nutrients from human urine to produce fertilizers can potentially benefit wastewater management and resource recovery strategies (Etter et al., 2011). However, high concentration of micropollutants in urine can accumulate in soil and plants and become hazardous (Khan and Nicell, 2010; Winker et al., 2010).

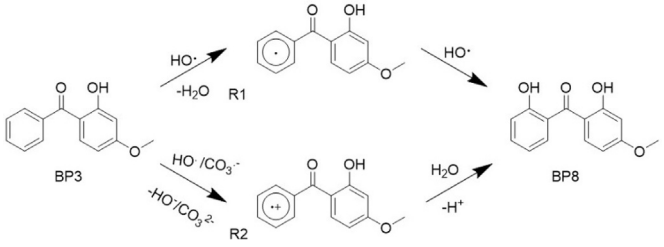

Scheme 1. BP8 formation mechanism about BP3 via HO·/$CO_3^{\cdot-}$ in the individual system during UV/H_2O_2 process (Noting: R1-Hydrogen Abstraction, R2-Electron Transfer).

Thus, the removal of micropollutants from urine becomes necessary for urine-based fertilizers. The removal of both pharmaceuticals and their metabolites (i.e., sulfamethoxazole, trimethoprim and N^4-acetylsulfamethoxazole) by AOPs in urine have been reported (Zhang et al., 2015). However, few studies have focused on the abatement of PCPs in urine, particularly for the frequent occurrence of UV filters (Cuderman and Heath, 2007; Meeker et al., 2013).

Compared with k_{obs} of BP via UV/H_2O_2 in ultrapure water, k_{obs} of BP1, BP3 and BP8 via UV/H_2O_2 in hydrolyzed urine decreased by 59.32, 86.77 and 90.53%, respectively, and followed the order of BP8 < BP3 < BP1 (Fig. 3A and S8). Kinetic modeling indicated that HO· concentration decreased from 5.00×10^{-12} M in ultrapure water to 1.62×10^{-15} M in hydrolyzed urine (Table 1). The decrease in HO· concentration was primarily due to competing reactions involving ammonia (NH_3) and HCO_3^-. The degradation of BP in hydrolyzed urine cannot be fully attributed to HO· (Table 1 and Fig. 3A), because k_{obs} should close to zero if the oxidation is governed only by HO·. These results suggested other reactive species contributed to BP degradation. High concentrations of NH_3, HCO_3^- and chloride (Cl^-) in hydrolyzed urine could be considered as sources for their corresponding radicals (Table 1).

Amino radical (·NH_2) would be initially generated from the reaction of NH_3 and HO· (No.102, Tables S3). Then, after a series of reactions with oxygen and H_2O_2, nitrogen dioxide radicals (·NO_2), nitric oxide radicals (·NO), ONOOH/$ONOO^-$ and a few other reactive intermediates would be produced. Although rate constants between reactive nitrogen species (RNS) and BP have not been previously determined, the reactions are expected because RNS are known to react with electron-rich aromatic moieties (Neta et al., 1978). ·NH_2 reacts with phenol and compounds with primary amine functional groups (i.e., *p*-aminophenol and *p*-phenylenediamine) (Neta et al., 1978), amino acids and melanins (Clarke et al., 2008). Given aromatic moieties (-OH as electron-donating group) of BP, they are likely to react with ONOOH, which could induce the nitration of naphthalene and benzene (Vione et al., 2005). The simulation results suggest that ·NO likely degrades BP to some extent because of its high concentration (2.32×10^{-5} M, Table 1). Although ·NH_2 concentration (3.37×10^{-13} M, Table 1) was low, identified byproducts suggests that ·NH_2 could react with BP. For instance, BP3, even *m*/*z* numbers (i.e., 228, 258, 280, 288 and 296) (Figure S9) indicate that generated transformation products (TPs) contained an odd number of nitrogen atoms. The exact mass information of TPs were illustrated by using LTQ-Orbitrap Velos Pro. Mass deviations of all proposed formulas were in the range of ±10 ppm of mass accuracy (Tables S4). Specifically, TP 228 (*m*/*z* 228, $C_{14}H_{14}NO_2$) implies that the −OH was replaced by $-NH_2$, which further oxidized to a nitro group TP 258 (*m*/*z* 258, $C_{14}H_{12}NO_4$).

The concentration of $CO_3^{\cdot-}$ in hydrolyzed urine (2.41×10^{-13} M, Table 1) decreased notably compared with that in surface water (1.44×10^{-11} M, Table 1). This decrease is primarily due to (i) both HCO_3^- and NH_3 competing to react with HO· and (ii) the combination reaction between $CO_3^{\cdot-}$ and ·NH_2. In addition, $CO_3^{\cdot-}$ concentration was inadequate to retain the significant degradation for BP. Furthermore, when Cl^- was not considered during simulations for hydrolyzed urine, HO· and $CO_3^{\cdot-}$ concentrations would be the same. Although the reaction rate of HO· with Cl^- is high (No.52, Table S3), a fast backward reaction (No.53, Table S3) also simultaneously occurs, leading to a stable HO· concentration. Hence, all the other RNS radicals generated from HO· would demonstrate negligible change due to Cl^- (Table S5). Meanwhile, when hydrolyzed urine without Cl^- was selected as a matrix, k_{obs} of BP was nearly identical to that in hydroxyl urine (Figure S10A). These results suggest that reactive chlorine species (RCS) did not contribute to BP degradation, because of its low concentrations (Table 1).

Compared with k_{obs} of BP by UV/PDS in ultrapure water, k_{obs} of BP1, BP3 and BP8 by UV/PDS in hydrolyzed urine decreased by 66.81, 90.37 and 88.54%, respectively, and followed the order of BP3 < BP8 < BP1 (Fig. 3B and S11). k_{obs} of BP1 and BP3 in hydrolyzed urine by UV/PDS were comparable to those in UV/H_2O_2 (Fig. 3). The quenching effect of NH_3 on $SO_4^{\cdot-}$ (No.103, Table S3) was lower than that on HO· (No.102, Table S3) due to the lower reaction rate. Thus, a significant concentration of $SO_4^{\cdot-}$, together with RNS, should have resulted in a greater removal rate for BP8 in UV/PDS; this rate was 1.56 times higher than that for UV/H_2O_2. Notably, ·NO_2 and ONOOH/$ONOO^-$ concentrations were much lower in UV/PDS than those in UV/H_2O_2, because H_2O_2 was essential in their generation process. In UV/PDS, hydrolyzed urine without Cl^- also negligibly affected k_{obs} for BP (Figure S10B). According to kinetic model, the decreased $SO_4^{\cdot-}$ concentration was mainly attributed to scavenging effect of Cl^- (No.54, Table S3). Unlike $ClOH^{\cdot-}$, generation of $SO_4^{\cdot-}$ from the reaction of chlorine atom ($Cl^{\cdot}$) and sulfate ion was slow due to low sulfate concentration and low reaction rate constant (No.55, Table S3) (Huie et al., 1991). Instead, the reaction of Cl· with H_2O and HO^- produced $ClOH^{\cdot-}$, which theoretically led to a higher HO· concentration, whereas the presence of HCO_3^- converted HO· to $CO_3^{\cdot-}$ (3.09×10^{-12} M for UV/PDS and 2.41×10^{-13} M for UV/H_2O_2, in Table 1). However, simulated radical concentrations could not fully account for the observed degradation rates in the experiments. This finding may be due to the overestimated scavenging effect of PDS on $CO_3^{\cdot-}$ (Yang et al., 2014).

In co-exposure pattern, degradation of individual contaminant obeyed pseudo-first-order kinetics (Figure S8D and S11D). Notably, BP3 degradation was strongly suppressed (only 6.06% and 5.69% of the overall degradation in UV/H_2O_2 and UV/PDS, respectively) (Fig. 3). This suppression is primarily attributed to molecular structure and RNS selectivity. In details, $-OCH_3$ group on BP3 inhibit RNS attraction due to steric hindrance and electron-drawing induction compare to BP1. Meanwhile, BP8 was more reactive than BP3, due to its electron-donating −OH on a different benzene ring (B.Smith and March 2007). The generated RNS were more prone to react with electron-rich sites (Neta et al., 1978). Simultaneously, byproducts formed from BP1 and/or BP8 via both AOPs during individual pattern could easily be attacked by RNS, owing to the lack of such discrepancy for BP3 and BP8. In particular, high selectivity of RNS played a critical role in the rapid degradation of BP1. In hydrolyzed urine, a similar tendency for co-exposure pattern via UV/H_2O_2 and UV/PDS was observed. This result implies that RNS, except for $CO_3^{\cdot-}$, exerted significant influence on the degradation behavior of BPs in hydrolyzed urine.

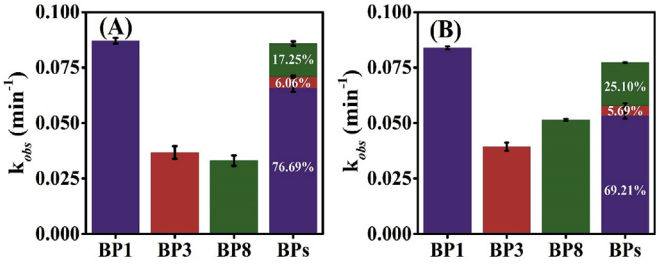

Fig. 3. Measured the degradation rate constants (k_{obs}) of BP1, BP3, BP8 and BPs in hydrolyzed urine at pH 9.2 by UV/H_2O_2 (A) and UV/PDS (B). Reaction condition: [BP1] = [BP3] = [BP8] = 5 μM, [H_2O_2] = [PDS] = 500 μM, $I = 1.99 \times 10^{-6}$ E L^{-1} s^{-1} and temperature at 25 ± 1 °C. Errors represent the standard deviation (n ≥ 2).

3.5. UV/H_2O_2 and UV/PDS AOPs in seawater

Various PCPs, including UV filters, are introduced by swimmers

into seawater. The concentrations of PCPs in seawater ranged the level from ng·L^{-1} to μg·L^{-1} (Díaz-Cruz et al., 2008; Ekowati et al., 2016; Giokas et al., 2007; Sun et al., 2014; Weng et al., 2014). The increase in popularity of by recreational activities in seawater, including swimming, snorkeling and scuba diving, brings the ubiquity of UV filters by extensive of visitors (Danovaro et al., 2008; Lamb et al., 2014). High reactivity of UV filters (i.e., BP3) with chlorine in bromide-rich seawater leads to the formation of chlorinated/brominated disinfection byproducts (Abdallah et al., 2015). To date, potential degradation of UV filters by UV-based AOPs in seawater has not been thoroughly investigated.

Compared with k_{obs} for BP degradation in ultrapure water, those for BP1, BP3 and BP8 degradation in seawater were reduced by 18.08, 86.20 and 90.96% for individual system via UV/H_2O_2, respectively (Fig. 4A and S12). Kinetic modeling indicated that HO· concentration decreased from 5.00×10^{-12} M in ultrapure water to 1.04×10^{-14} M in seawater (Table 1). The decrease of HO· concentration was primarily due to competing anions, including Cl^-, HCO_3^- and bromide (Br^-). The modeling HO· concentrations in seawater without Cl^-, HCO_3^- and Br^- was 6.55×10^{-14}, 1.06×10^{-14} and 1.77×10^{-12} M, respectively (Table S6). Results indicated that Br^- was the sink for HO·, highlighting the important role of Br^- despite its low concentration relative to that of Cl^-. Hence, conversion of HO· to less-reactive halogen species (RHS) and $CO_3^{\cdot-}$ was responsible for k_{obs} decrease. The degradation rate followed the order BP8 < BP3 < BP1 (Fig. 4A). Likewise, k_{obs} should close to zero if the oxidation by only HO· was considered. High concentration of Cl^- in seawater guaranteed an abundance of its corresponding radical (Table 1). The generated RHS, including Cl· and $Cl_2^{\cdot-}$, favored $CO_3^{\cdot-}$ generation. Compared with BP3 or BP8, high selectivity of RHS for BP1 may responsible for its eminent degradation because $k_{CO_3^{\cdot-}}$ was still of the same order of magnitude (Table 2).

Compared with k_{obs} for BP in ultrapure water, those for BP1, BP3 and BP8 in seawater were reduced by 17.76, 54.44 and 58.73% for individual systems via UV/PDS, respectively (Fig. 4B and S13). Similarly, conversion of HO· and $SO_4^{\cdot-}$ to RHS and $CO_3^{\cdot-}$ was responsible for k_{obs} decrease. In UV/PDS, k_{obs} of BP were higher than those in UV/H_2O_2, especially for BP3 and BP8 (Fig. 4B). Likewise, k_{obs} for all BP should close to zero if the oxidation only dominated by $SO_4^{\cdot-}$ and HO·. $CO_3^{\cdot-}$ should not be responsible for the significant degradation improvement for BP3 and BP8 (Fig. 4) because its concentration was decreased by 15 times (1.22×10^{-10} M for UV/H_2O_2 and 7.87×10^{-12} M for UV/PDS, Table 1). Furthermore, comparison of RHS concentrations between UV/H_2O_2 and UV/PDS were performed. The concentrations of halogen radicals, including Cl·, $Cl_2^{\cdot-}$, Br·, $Br_2^{\cdot-}$ and $BrCl^{\cdot-}$, in UV/PDS were 2–10 times higher than those in UV/H_2O_2. The concentration of ClO· was 9 orders of magnitude higher in UV/PDS than UV/H_2O_2 (Table 1). Unlike UV/H_2O_2, the concentration of $SO_4^{\cdot-}$ for UV/PDS without Cl^-, HCO_3^- and Br^- barely reached those levels in ultrapure water (Table S6). Surprisingly, when Cl^- and Br^- were absent, $SO_4^{\cdot-}$ concentration was nearly identical to that observed in ultrapure water. This similarity demonstrates that coexistence of Cl^- and Br^- was the sink for $SO_4^{\cdot-}$. Nevertheless, HO· concentration from modeling calculation was 4.6 times lower than that in ultrapure water due to the presence of HCO_3^-. The enhanced degradation in UV/PDS compared to UV/H_2O_2 may stem from higher RHS concentrations. Until now, identification of the halogen radical(s) accounting for improvement of BP degradation was still unclear.

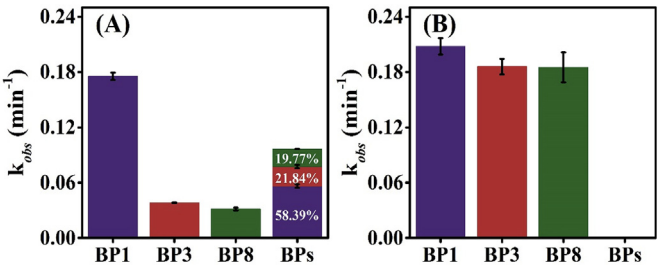

Fig. 4. Measured the degradation rate constants (k_{obs}) of BP1, BP3, BP8 and BPs in seawater at pH 7.6 by UV/H_2O_2 (A) and UV/PDS (B). Reaction condition: [BP1] = [BP3] = [BP8] = 5 μM, [H_2O_2] = [PDS] = 500 μM, $I = 1.99 \times 10^{-6}$ E L^{-1} s^{-1} and temperature at 25 ± 1 °C. Errors represent the standard deviation (n ≥ 2). Note: The co-exposure degradation behavior of BPs in seawater were shown in Figure S14.

With respect to co-exposure pattern in seawater, UV/H_2O_2 for BPs followed pseudo-first-order kinetics and exhibited similar degradation tendency as individual system (Figure S12D and 4A). Similarly, degradation of BP1 via UV/PDS was consistent with pseudo-first-order kinetics (Figure S14A). However, degradation of BP3 and BP8 via UV/PDS displayed biphasic kinetics (Figure S14B, C). Specifically, their degradation was initially slow (a lag phase), followed by a rapid secondary decay phase. These results imply that the capability of RHS contributing to degradation of investigated compounds was different. Moreover, non-first-order degradation of co-exposure micropollutants by UV/PDS has not been previously reported. Currently, elucidation of non-first-order degradation behavior is difficult. As we observed, the contribution of RHS for BP3 and BP8 rarely occurred until BP1 had decreased by certain level (89.30% for BP3 and 73.84% for BP8). This phenomenon was due to a higher selectivity of RHS for BP1 than BP3 and BP8. Furthermore, occurrence of an accelerating stage (ca. 25 min for BP3 and 15 min for BP8) may due to the differences in molecular structure besides *m*-methoxyphenol. A higher electron-donor character of phenol/phenolate functional group favors the electrophilic attack of chlorine or bromine (Deborde and Von Gunten, 2008). This finding might provide the insight knowledge to unravel non-first-order behavior in co-exposure pattern. RHS investigation based on radical reactions in seawater are much more complicated than those in ultrapure water; future work should utilize this type of investigation to elucidate such degradation behavior.

In summary, degradation behaviors of target contaminants depend on (i) their molecular structure, (ii) operable UV-based AOPs, (iii) matrix constituents, and (iv) feeding patterns (individual or co-exposure). Molecular properties, such as geometric configuration and charge distribution, would be the intrinsic factor for degradation behaviors. HO· and $SO_4^{\cdot-}$ are the reactive species source during UV/H_2O_2 and UV/PDS processes, respectively. Constituents (i.e., HCO_3^-, NH_3, Cl^- and Br^-) and their concentrations in water matrix affect conversion of reactive species, which complicates the elimination of contaminants. Notably, the reaction between reactive species (i.e., RNS and RHS) and parent compounds can generate various byproducts, and elucidating their mechanisms requires further study. In particular, because benzophenone derivatives frequently co-exist in aqueous environments, examination on co-exposure pattern is more practical and can benefit the overall understanding of their abatement. Furthermore, mechanism of interference from generated byproducts and non-first-order behavior also warrants further investigation. Compared with those in ultrapure water, degradation efficiency on BP for UV/H_2O_2 and UV/PDS in real matrices was decreased by various extents (17.76–90.96%). Accordingly, economic analysis regarding BP degradation is necessary to facilitate the selection of a cost-efficient treatment.

3.6. Economic analysis using EE/O

To compare AOPs for BP degradation in different water matrices

(surface water, hydrolyzed urine and seawater), an economic analysis using electrical efficiency per log order (EE/O) concept was further conducted. Details about calculation of EE/O were described in the Text S3.

In this study, EE/O_{total} was calculated based on 90% of target compounds removal. As shown in Table 3, UV/H_2O_2 was more cost-effective treatment than UV/PDS when BP degradation happened in ultrapure water, surface water and hydrolyzed urine (except for BP8). This was primarily because PDS was more expensive than H_2O_2. Nevertheless, UV/PDS process costs less energy than UV/H_2O_2 process in seawater (except for BP1), which ascribe to the higher concentration of RHS as we discussed in section 3.5. Regardless of UV/H_2O_2 and UV/PDS, it was generally less effective in synthetic matrices than in ultrapure water. For example, at the molar fraction of oxidant/BP3 = 100, the EE/O_{total} for the UV/H_2O_2 in ultrapure water is 0.63×10^{-3} kWh·L^{-1}, which is 1.87, 6.38 and 6.13 times lower that in surface water (1.18×10^{-3} kWh·L^{-1}), hydrolyzed urine (4.02×10^{-3} kWh·L^{-1}) and seawater (3.86×10^{-3} kWh·L^{-1}), respectively. Similarly, the EE/O_{total} for BP3 elimination via UV/PDS in ultrapure water is 1.62×10^{-3} kWh·L^{-1}, which is 2.72, 3.04 and 1.26 times lower that in surface water (4.41×10^{-3} kWh·L^{-1}), hydrolyzed urine (4.92×10^{-3} kWh·L^{-1}) and seawater (2.04×10^{-3} kWh·L^{-1}), respectively. These results further demonstrate that constituents of water matrices can greatly affect the efficiency of AOPs for contaminants removal.

4. Conclusions

The individual and co-exposure patterns of benzophenone derivatives degradation using UV/H_2O_2 and UV/PDS were investigated under various water matrices. The following conclusions were obtained:

(1) Benzophenone derivatives could be degraded by HO•, $SO_4^{\bullet-}$ and $CO_3^{\bullet-}$, and the second-order rate constants were determined (Table 2).
(2) In surface water, attack of BP3 by HO• and $CO_3^{\bullet-}$ in UV/H_2O_2 can generate BP8, which was responsible for the relatively high degradation rate of BP3. Intermediates generated from BP3 and BP8 in UV/PDS were susceptible to $CO_3^{\bullet-}$, which resulting in the reduction for BP1 degradation.
(3) In hydrolyzed urine, Cl^- was shown the negligible for benzophenone derivatives degradation due to low concentration of RCS. BP3 abatement was excessively inhibited during co-exposure pattern for both AOPs.
(4) In seawater, non-first-order kinetic behavior for BP3 and BP8 was found during co-exposure pattern. Br^- was the sink of HO•, and the co-existence of Br^- and Cl^- was the sink of $SO_4^{\bullet-}$.
(5) In terms of energy efficiency, UV/H_2O_2 process is usually more economically competitive than UV/PDS process.

We holistically evaluated the performance of two typical AOPs (UV/H_2O_2 and UV/PDS), which depended on (i) molecular structure of contaminants, (ii) components of water matrices and (iii) reactive radical species. Kinetic simulations conducted in this study provided a trend comparison of radical concentrations under different conditions. Results illustrated the variation of main reactive species and unraveled the differences in AOPs. Meanwhile, due to the coexistence and interference of benzophenone derivatives, their degradation becomes more complicated. Hence, a comprehensive evaluation of AOPs performance for micropollutants destroying in natural matrices is urgently needed. Our findings will trigger further investigation regarding other types of micropollutants in mixed systems using UV-based AOPs.

Table 3
EE/O values[a] for UV/H_2O_2 and UV/PDS treatment of BP in different water matrices (in 10^{-3} kWh·L^{-1}).

Water Matrix		BP1	BP3	BP8
Ultrapure water	UV/H_2O_2	0.78	0.63	0.53
	UV/PDS	1.84	1.62	1.59
Surface water	UV/H_2O_2	1.36	1.18	1.10
	UV/PDS	2.35	4.41	4.12
Hydrolyzed urine	UV/H_2O_2	1.76	4.02	4.46
	UV/PDS	2.98	4.92	4.06
Seawater	UV/H_2O_2	0.93	3.86	4.67
	UV/PDS	1.96	2.04	2.05

[a] Calculated EE/O values were applied for the following experiment conditions: UV fluence rate = 1.99×10^{-6} E L^{-1} s^{-1}, $[H_2O_2] = [PDS] = 0.5$ mM, [BP1] = [BP3] = [BP8] = 5.0 μM.

Acknowledgments

This work was supported by the National Natural Science Foundation of China (51478171, and 51778218). The authors appreciate the support from the Brook Byers Institute for Sustainable Systems, Hightower Chair and Georgia Research Alliance at the Georgia Institute of Technology. The views and ideas expressed herein are solely those of the authors and do not represent the ideas of the funding agencies in any form. We also thank ChemWorx for English editing.

Appendix A. Supplementary data

Supplementary data to this article can be found online at https://doi.org/10.1016/j.watres.2019.05.019.

Declaration of interests

The authors declare that they have no known competing financial interests or personal relationships that could have appeared to influence the work reported in this paper.

References

Abdallah, P., Deborde, M., Dossier Berne, F., Karpel Vel Leitner, N., 2015. Kinetics of chlorination of benzophenone-3 in the presence of bromide and ammonia. Environ. Sci. Technol. 49 (24), 14359–14367.
Asimakopoulos, A.G., Thomaidis, N.S., Kannan, K., 2014. Widespread occurrence of bisphenol A diglycidyl ethers, p-hydroxybenzoic acid esters (parabens), benzophenone type-UV filters, triclosan, and triclocarban in human urine from Athens, Greece. Sci. Total Environ. 470–471 (2), 1243–1249.
Balmer, M.E., Buser, H.-R., Müller, Markus D., Poiger, T., 2005. Occurrence of some organic UV filters in wastewater, in surface waters, and in fish from Swiss lakes. Environ. Sci. Technol. 39 (4), 953–962.
Baxendale, J.H., Wilson, J.A., 1957. The photolysis of hydrogen peroxide at high light intensities. Trans. Faraday Soc. 53, 344–356.
Beltrán, F.J., Ovejero, G., Garciaaraya, J.F., Rivas, J., 1995. Oxidation of polynuclear aromatic-hydrocarbons in water .2. UV-Radiation and ozonation in the presence of UV-radiation. Ind. Eng. Chem. Res. 34, 1607–1615.
Brausch, J.M., Rand, G.M., 2011. A review of personal care products in the aquatic environment: environmental concentrations and toxicity. Chemosphere 82 (11), 1518–1532.
Brezonik, P.L., Fulkerson-Brekken, J., 1998. Nitrate-induced photolysis in natural waters: controls on concentrations of hydroxyl radical photo-intermediates by natural scavenging agents. Environ. Sci. Technol. 32 (19), 3004–3010.
Canonica, S., Kohn, T., Mac, M., Real, F.J., Wirz, J., von Gunten, U., 2005. Photosensitizer method to determine rate constants for the reaction of carbonate radical with organic compounds. Environ. Sci. Technol. 39 (23), 9182–9188.
Castro, G., Casado, J., Rodríguez, I., Ramil, M., Ferradás, A., Cela, R., 2016. Time-of-flight mass spectrometry assessment of fluconazole and climbazole UV and UV/H_2O_2 degradability: kinetics study and transformation products elucidation. Water Res. 88, 681–690.
Clarke, K., Edge, R., Johnson, V., Land, E., Navaratnam, S., Truscott, T., 2008. Direct observation of NH_2• reactions with oxygen, amino acids, and melanins. J. Phys. Chem. A 112 (6), 1234–1237.

Cuderman, P., Heath, E., 2007. Determination of UV filters and antimicrobial agents in environmental water samples. Anal. Bioanal. Chem. 387 (4), 1343–1350.
Danovaro, R., Bongiorni, L., Corinaldesi, C., Giovannelli, D., Damiani, E., Astolfi, P., Greci, L., Pusceddu, A., 2008. Sunscreens cause coral bleaching by promoting viral infections. Environ. Health Perspect. 116 (4), 441–447.
Deborde, M., Von Gunten, U., 2008. Reactions of chlorine with inorganic and organic compounds during water treatment-kinetics and mechanisms: a critical review. Water Res. 42 (1), 13–51.
Díaz-Cruz, M.S., Llorca, M., Barceló, D., 2008. Organic UV filters and their photodegradates, metabolites and disinfection by-products in the aquatic environment. Trac. Trends Anal. Chem. 27 (10), 873–887.
Ekowati, Y., Buttiglieri, G., Ferrero, G., Valle-Sistac, J., Diaz-Cruz, M.S., Barceló, D., Petrovic, M., Villagrasa, M., Kennedy, M.D., Rodríguez-Roda, I., 2016. Occurrence of pharmaceuticals and UV filters in swimming pools and spas. Environ. Sci. Pollut. Res. 23 (14), 14431–14441.
Etter, B., Tilley, E., Khadka, R., Udert, K.M., 2011. Low-cost struvite production using source-separated urine in Nepal. Water Res. 45 (2), 852–862.
Feng, S., Zhang, X., Liu, Y., 2015. New insights into the primary phototransformation of acetaminophen by UV/H_2O_2: photo-Fries rearrangement versus hydroxyl radical induced hydroxylation. Water Res. 86, 35–45.
Fent, K., Zenker, A., Rapp, M., 2010. Widespread occurrence of estrogenic UV-filters in aquatic ecosystems in Switzerland. Environ. Pollut. 158 (5), 1817–1824.
Giokas, D.L., Salvador, A., Chisvert, A., 2007. UV filters: from sunscreens to human body and the environment. Trac. Trends Anal. Chem. 26 (5), 360–374.
Huie, R.E., Clifton, C.L., Neta, P., 1991. Electron transfer reaction rates and equilibria of the carbonate and sulfate radical anions. Radiat. Phys. Chem. 38 (38), 477–481.
Ianni, J.C., 2012. Windows Version 4.55. www.kintecus.com.
Jansen, R., Osterwalder, U., Wang, S.Q., Burnett, M., Lim, H.W., 2013. Photoprotection: part II. Sunscreen: development, efficacy, and controversies. J. Am. Acad. Dermatol. 69 (6), 867.e861-867.e814.
Kasprzyk-Hordern, B., Dinsdale, R.M., Guwy, A.J., 2008. The occurrence of pharmaceuticals, personal care products, endocrine disruptors and illicit drugs in surface water in South Wales, UK. Water Res. 42 (13), 3498–3518.
Kasprzyk-Hordern, B., Dinsdale, R.M., Guwy, A.J., 2009. The removal of pharmaceuticals, personal care products, endocrine disruptors and illicit drugs during wastewater treatment and its impact on the quality of receiving waters. Water Res. 43 (2), 363–380.
Keen, O.S., Linden, K.G., 2013. Degradation of antibiotic activity during UV/H_2O_2 advanced oxidation and photolysis in wastewater effluent. Environ. Sci. Technol. 47 (22), 13020–13030.
Khan, U., Nicell, J.A., 2010. Assessing the risk of exogenously consumed pharmaceuticals in land-applied human urine. Water Sci. Technol. 62 (6), 1335–1345.
Kim, S., Choi, K., 2014. Occurrences, toxicities, and ecological risks of benzophenone-3, a common component of organic sunscreen products: a mini-review. Environ. Int. 70, 143–157.
Kunisue, T., Chen, Z., Buck Louis, G.M., Sundaram, R., Hediger, M.L., Sun, L., Kannan, K., 2012. Urinary concentrations of benzophenone-type UV filters in US women and their association with endometriosis. Environ. Sci. Technol. 46 (8), 4624–4632.
Lamb, J.B., True, J.D., Piromvaragorn, S., Willis, B.L., 2014. Scuba diving damage and intensity of tourist activities increases coral disease prevalence. Biol. Conserv. 178, 88–96.
Li, W., Ma, Y., Guo, C., Hu, W., Liu, K., Wang, Y., Zhu, T., 2007. Occurrence and behavior of four of the most used sunscreen UV filters in a wastewater reclamation plant. Water Res. 41 (15), 3506–3512.
Liu, Y.S., Ying, G.G., Shareef, A., Kookana, R.S., 2011. Photostability of the UV filter benzophenone-3 and its effect on the photodegradation of benzotriazole in water. Environ. Chem. 8 (6), 581–588.
Liu, Y., He, X., Duan, X., Fu, Y., Dionysiou, D.D., 2015. Photochemical degradation of oxytetracycline: influence of pH and role of carbonate radical. Chem. Eng. J. 276, 113–121.
Liu, T., Yin, K., Liu, C., Luo, J., Crittenden, J., Zhang, W., Luo, S., He, Q., Deng, Y., Liu, H., 2018. The role of reactive oxygen species and carbonate radical in oxcarbazepine degradation via UV, UV/H_2O_2: kinetics, mechanisms and toxicity evaluation. Water Res. 147, 204–213.
Luo, C., Ma, J., Jiang, J., Liu, Y., Song, Y., Yang, Y., Guan, Y., Wu, D., 2015. Simulation and comparative study on the oxidation kinetics of atrazine by UV/H_2O_2, UV/HSO_5^- and UV/$S_2O_8^{2-}$. Water Res. 80, 99–108.
Luo, C., Jiang, J., Guan, C., Ma, J., Pang, S., Song, Y., Yang, Y., Zhang, J., Wu, D., Guan, Y., 2017. Factors affecting formation of deethyl and deisopropyl products from atrazine degradation in UV/H_2O_2 and UV/PDS. RSC Adv. 7 (46), 29255–29262.
Magi, E., Scapolla, C., Carro, M.D., Rivaro, P., Nguyen, K.T.N., 2013. Emerging pollutants in aquatic environments: monitoring of UV filters in urban wastewater treatment plants. Anal. Methods-UK. 5 (2), 428–433.
Manasfi, T., Storck, V., Ravier, S., Demelas, C., Coulomb, B., Boudenne, J.-L., 2015. Degradation products of benzophenone-3 in chlorinated seawater swimming pools. Environ. Sci. Technol. 49 (15), 9308–9316.
Manasfi, T., Coulomb, B., Ravier, S., Boudenne, J.L., 2017. Degradation of organic UV filters in chlorinated seawater swimming pools: transformation pathways and bromoform formation. Environ. Sci. Technol. 51 (23), 13580–13591.
Mark, G., Schuchmann, M.N., Schuchmann, H.-P., von Sonntag, C., 1990. The photolysis of potassium peroxodisulphate in aqueous solution in the presence of tert-butanol: a simple actinometer for 254 nm radiation. J. Photochem. Photobiol. A Chem. 55 (2), 157–168.
Meeker, J.D., Cantonwine, D.E., Rivera-González, L.O., Ferguson, K.K., Mukherjee, B., Calafat, A.M., Ye, X., Liza, V., A.D.T, Crespo-Hernández, N., Jiménez-Vélez, B., Alshawabkeh, A.N., Cordero, J.F., 2013. Distribution, variability and predictors of urinary concentrations of phenols and parabens among pregnant women in Puerto Rico. Environ. Sci. Technol. 47 (7), 3439–3447.
Nakagawa, Y., Suzuki, T., 2002. Metabolism of 2-hydroxy-4-methoxybenzophenone in isolated rat hepatocytes and xenoestrogenic effects of its metabolites on MCF-7 human breast cancer cells. Chem. Biol. Interact. 139 (2), 115–128.
Negreira, N., Rodríguez, I., Ramil, M., Rubí, E., Cela, R., 2009. Sensitive determination of salicylate and benzophenone type UV filters in water samples using solid-phase microextraction, derivatization and gas chromatography tandem mass spectrometry. Anal. Chim. Acta 638 (1), 36–44.
Neta, P., Maruthamuthu, P., Carton, P.M., Fessenden, R.W., 1978. Formation and reactivity of the amino radical. J. Phys. Chem. 82 (17), 1875–1878.
Nfodzo, P., Choi, H., 2011. Sulfate radicals destroy pharmaceuticals and personal care products. Environ. Eng. Sci. 28 (8), 605–609.
Oller, I., Malato, S., Sánchez-Pérez, J.A., 2011. Combination of Advanced Oxidation Processes and biological treatments for wastewater decontamination-a review. Sci. Total Environ. 409 (20), 4141–4166.
Oturan, M.A., Aaron, J.-J., 2014. Advanced oxidation processes in water/wastewater treatment: principles and applications. A review. Crti. Rev. Eni. Sci. Tec 44 (23), 2577–2641.
Philippat, C., Mortamais, M., Chevrier, C., Petit, C., Calafat, A.M., Ye, X., Silva, M.J., Brambilla, C., Pin, I., Charles, M.A., Cordier, S., Rémy, S., 2012. Exposure to phthalates and phenols during pregnancy and offspring size at birth. Environ. Health Perspect. 120 (3), 464–470.
Poiger, T., Buser, H.-R., Balmer, M.E., Bergqvist, P.-A., Müller, M.D., 2004. Occurrence of UV filter compounds from sunscreens in surface waters: regional mass balance in two Swiss lakes. Chemosphere 55 (7), 951–963.
Rubio, D., Casanueva, J.F., Nebot, E., 2013. Improving UV seawater disinfection with immobilized TiO_2: study of the viability of photocatalysis (UV254/TiO_2) as seawater disinfection technology. J. Photochem. Photobiol. A Chem. 271, 16–23.
Schlumpf, M., Cotton, B., Conscience, M., Haller, V., Steinmann, B., Lichtensteiger, W., 2001. In vitro and in vivo estrogenicity of UV screens. Environ. Health Perspect. 109 (3), 239–244.
Schreurs, R., Lanser, P., Seinen, W., Van, d.B.B., 2002. Estrogenic activity of UV filters determined by an in vitro reporter gene assay and an in vivo transgenic zebrafish assay. Arch. Toxicol. 76 (5–6), 257–261.
Schreurs, R.H.M.M., Sonneveld, E., Jansen, J.H.J., Seinen, W., Van, d.B.B., 2005. Interaction of polycyclic musks and UV filters with the estrogen receptor (ER), androgen receptor (AR), and progesterone receptor (PR) in reporter gene bioassays. Toxicol. Sci. 83 (2), 264–272.
Smith, B., M, March, J., 2007. March's Advanced Organic Chemistry: Reactions, Mechanisms, and Structure. John Wiley & Sons.
Sun, Q., Lv, M., Hu, A., Yang, X., Yu, C.-P., 2014. Seasonal variation in the occurrence and removal of pharmaceuticals and personal care products in a wastewater treatment plant in Xiamen, China. J. Hazard Mater. 277 (4), 69–75.
Sun, P., Lee, W.-N., Zhang, R., Huang, C.-H., 2016. Degradation of DEET and caffeine under UV/chlorine and simulated sunlight/chlorine conditions. Environ. Sci. Technol. 50 (24), 13265–13273.
Suzuki, T., Kitamura, S., Khota, R., Sugihara, K., Fujimoto, N., Ohta, S., 2005. Estrogenic and antiandrogenic activities of 17 benzophenone derivatives used as UV stabilizers and sunscreens. Toxicol. Appl. Pharmacol. 203 (1), 9–17.
Tang, R., Chen, M.J., Ding, G.D., Chen, X.J., Han, X.M., Zhou, K., Chen, L.M., Xia, Y.K., Tian, Y., Wang, X.R., 2013. Associations of prenatal exposure to phenols with birth outcomes. Environ. Pollut. 178 (1), 115–120.
Tsui, M.M.P., Leung, H.W., Wai, T.-C., Yamashita, N., Taniyasu, S., Liu, W., Lam, P.K.S., Murphy, M.B., 2014. Occurrence, distribution and ecological risk assessment of multiple classes of UV filters in surface waters from different countries. Water Res. 67, 55–65.
Tsui, M.M.P., Lam, J.C.W., Ng, T.Y., Ang, P.O., Murphy, M.B., Lam, P.K.S., 2017. Occurrence, distribution and fate of organic UV filters in coral communities. Environ. Sci. Technol. 51 (8), 4182–4190.
Vione, D., Maurino, V., Minero, C., Pelizzetti, E., 2005. Nitration and photonitration of naphthalene in aqueous systems. Environ. Sci. Technol. 39 (4), 1101–1110.
Wang, L., Kannan, K., 2013. Characteristic profiles of benzonphenone-3 and its derivatives in urine of children and adults from the United States and China. Environ. Sci. Technol. 47 (21), 12532–12538.
Weng, S.C., Sun, P., Ben, W., Huang, C.-H., Lee, L.T., Blatchley III, E.R., 2014. The presence of pharmaceuticals and personal care products in swimming pools. Environ. Sci. Technol. Lett. 1 (12), 495–498.
Winker, M., Clemens, J., Reich, M., Gulyas, H., Otterpohl, R., 2010. Ryegrass uptake of carbamazepine and ibuprofen applied by urine fertilization. Sci. Total Environ. 408 (8), 1902–1908.
Wols, B.A., Hofman-Caris, C.H.M., 2012. Review of photochemical reaction constants of organic micropollutants required for UV advanced oxidation processes in water. Water Res. 46 (9), 2815–2827.
Wols, B.A., Harmsen, D.J.H., Beerendonk, E.F., Hofman-Caris, C.H.M., 2015. Predicting pharmaceutical degradation by UV (MP)/H_2O_2 processes: a kinetic model. Chem. Eng. J. 263 (6), 336–345.
Wu, J.W., Chen, H.C., Ding, W.H., 2013. Ultrasound-assisted dispersive liquid–liquid microextraction plus simultaneous silylation for rapid determination of salicylate and benzophenone-type ultraviolet filters in aqueous samples. J. Chromatogr. A 1302, 20–27.
Yang, Y., Pignatello, J.J., Ma, J., Mitch, W.A., 2014. Comparison of halide impacts on

the efficiency of contaminant degradation by sulfate and hydroxyl radical-based advanced oxidation processes (AOPs). Environ. Sci. Technol. 48 (4), 2344–2351.
Yang, L.M., Chen, Z.L., Cui, D., Luo, X.B., Liang, B., Yang, L.X., Liu, T., Wang, A.J., Luo, S.L., 2019. Ultrafine palladium nanoparticles supported on 3D self-supported Ni foam for cathodic dechlorination of florfenicol. Chem. Eng. J. 359, 894–901.
Yao, H., Sun, P., Minakata, D., Crittenden, J.C., Huang, C.-H., 2013. Kinetics and modeling of degradation of ionophore antibiotics by UV and UV/H_2O_2. Environ. Sci. Technol. 47 (9), 4581–4589.
Yin, K., Deng, L., Luo, J., Crittenden, J.C., Liu, C., Wei, Y., Wang, L., 2018. Destruction of phenicol antibiotics using the UV/H_2O_2 process: kinetics, byproducts, toxicity evaluation and trichloromethane formation potential. Chem. Eng. J. 351, 867–877.
Zhang, R., Sun, P., Boyer, T.H., Zhao, L., Huang, C.-H., 2015. Degradation of pharmaceuticals and metabolite in synthetic human urine by UV, UV/H_2O_2, and UV/PDS. Environ. Sci. Technol. 49 (5), 3056–3066.
Zhang, R., Yang, Y., Huang, C.-H., Zhao, L., Sun, P., 2016a. Kinetics and modeling of sulfonamide antibiotic degradation in wastewater and human urine by UV/H_2O_2 and UV/PDS. Water Res. 103, 283–292.
Zhang, R.C., Yang, Y.K., Huang, C.H., Li, N., Liu, H., Zhao, L., Sun, P.Z., 2016b. UV/H_2O_2 and UV/PDS treatment of trimethoprim and sulfamethoxazole in synthetic human urine: transformation products and toxicity. Environ. Sci. Technol. 50 (5), 2573–2583.